Physics Faculty Research & Creative Works

Physics

01 Jan 2014

Interaction of Positrons and Electrons with Atoms

Robert D. DuBois

Missouri University of Science and Technology, dubois@mst.edu

PURPOSE-LED
PUBLISHING™

Interaction of positrons and electrons with atoms

To cite this article: R D DuBois 2014 *J. Phys.: Conf. Ser.* **488** 012054

View the article online for updates and enhancements.

Interaction of positrons and electrons with atoms

R D DuBois

Department of Physics, Missouri University of Science and Technology, Rolla, MO 65409 USA

dubois@mst.edu

Abstract. Progress in differential studies of ionization resulting from positron and electron impact being performed at the Missouri University of Science and Technology is described. Examples of doubly and triply (fully) differential single ionization data for the ejected electron and the scattered projectile channels are presented. Energy loss data for double ionization, plus estimates for the first-order interaction, shake off, SO, and TS1, are also presented.

1. Introduction

As a charged particle passes by an atom the bound electrons are subjected to coulomb forces from the projectile nucleus and, for dressed projectiles, from any projectile electrons. Depending on whether the projectile has a net positive charge, i.e., positive ions and positrons, or a net negative charge, i.e., negative ions, electrons and antiprotons, the force is either attractive or repulsive. The probability that these bound electrons are ionized (or excited) is proportional to the square of the net coulomb force integrated over the time of the interaction. Therefore, for single electron removal of an outer shell electron by bare $Z=1$ particles and antiparticles, e.g., positrons, electrons, protons and antiprotons, first order perturbation theories such as the first Born approximation predict identical total cross sections for fast isotachic collisions. For multiple electron removal the situation is more complicated as different channels can contribute and interfere.[1]

On the other hand, on the differential level, single ionization cross sections can differ for particle and antiparticle impact due to the attractive/repulsive nature of the coulomb force associated with the sign of the projectile charge. This can produce polarization effects where the target electron cloud is pulled toward the projectile for positron and proton impact or partially repulsed for electron and antiproton impact. These polarization effects will lead to increased or decreased cross sections depending on the sign of the projectile charge. The attractive/repulsive coulomb forces can also lead to projectile trajectory effects, e.g., larger or smaller impact parameters, again depending on the sign of the projectile charge. This again influences the magnitude of the ionization cross section but also will alter the energy distributions of the ionized electrons and scattered projectiles since smaller impact parameters generate higher energy transfers. In addition, the ionized electron trajectories can be influenced by coulomb attractions/repulsions by the exiting projectile. Typically, the more highly differential the measurement, the greater these differences associated with the sign of the projectile charge can be. Since the advent of atomic collision physics, numerous comparisons of proton and electron impact data have been made to investigate such effects. But interpreting these comparisons is complicated by additional effects due to the vastly different projectile masses.

A less ambiguous comparison employs comparisons of particle and antiparticle data, e.g., electron-positron or proton-antiproton comparisons, since here only a single parameter, namely the sign of the charge, changes. Although great advances have been made in the two decades with regard to total cross section comparisons for antiproton and proton impact, see ref. 2 for example, differential measurements using antiprotons are still beyond experimental capabilities. Likewise, until our work at the Missouri University of Science and Technology differential data for positron impact were sparce, see ref. 3 and 4 and references therein. In order to help fill this void, our experimental program studies and compares ionization resulting from positron and electron impact with particular emphasis on highly differential studies of the target electron emission and the projectile scattering.

2. Method

Figure 1 shows a schematic diagram of the experimental apparatus being used. The basic method involves crossing a beam of positrons or electrons with a simple gas jet emerging from a hypodermic needle positioned between two biased plates. A weak electric field between the plates extracts target ions produced in the beam-gas jet interaction volume. These target ions exit the target region through an aperture, pass through a short time-of-flight spectrometer, and are detected by a channeltron. Using these ions as an "ionization event trigger" discriminates against interactions occurring outside the interaction volume plus provides information about the target ion charge and mass ratio. It also allows us to remove background gas contributions and to isolate single and multiple ionization events.

Immediately following the target region is a specially designed electrostatic spectrometer and a position-sensitive channelplate for detecting forward scattered projectiles as a function of their post-collision energy and scattering angle. Detector size and distance from the interaction region allows us to study scattering angles less than ~5° and energy loss ranges that are ~ 20% of the beam energy. Directly above the top biased plate is a second position-sensitive channelplate used to detect ejected electrons. This detector is placed as close as possible, making it sensitive to geometric emission angles between 30° and 150°. In order to obtain sufficient statistics for positron impact, large beam diameters, ~5-6 mm, are used. This means that ionization occurs within an extended volume, rather than at a single point. In addition, the electric field used to extract target ions influences the

Figure 1. Schematic of MS&T positron and electron differential ionization apparatus showing the recoil ion, scattered projectile, and ejected electron detectors, the target region and the projectile spectrometer. The boxes and the arrows show which detector signals are used in coincidence for various types of studies.

electron trajectories, particularly for low energy electrons. Thus, the emission angles vary with electron energy and only for higher energy emission do they correspond to the geometric angles. Therefore, a downside of this method is that to compare our data with theory, a detailed convolution of theory over the experimental geometry and electric fields is necessary. On the other hand, a major strength of our method is that both positron and electron impact measurements are performed using the same apparatus and that doubly and triply differential data for multiple as well as single ionization data are all obtained simultaneously. Hence, systematic errors associated with comparing the various types of data are minimized. For a full description of the apparatus and methods, the reader is referred to ref. 4.

Various combinations of coincidences between the three detectors, as illustrated in Fig. 1, allow us to measure singly, doubly, and triply (or fully) differential cross sections (yields) which throughout this article will be identified by SDCS, DDCS, and TDCS (or FDCS). Figure 2 shows examples of a
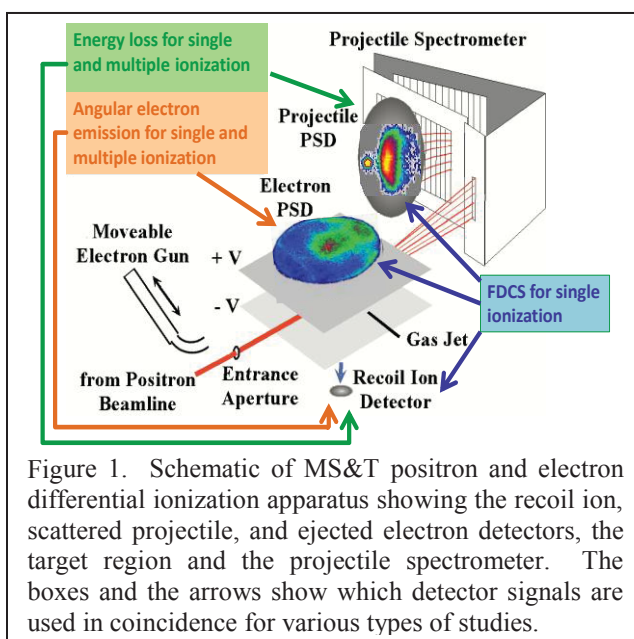
scattered projectile 2D spectrum, a time-of-flight target ion spectrum, and an ejected electron spectrum, top row, plus DDCS and TDCS 2D scattered projectile spectra for 200 eV electron and positron impact single ionization of argon, middle and bottom rows. To obtain the DDCS spectra (middle and bottom rows, left figures), the scattered projectile (upper left) and single ionization peak in the recoil ion time-of-flight spectrum (upper middle) are combined; adding an additional coincidence with the ejected electron signal (upper right) produces TDCS spectra (middle and bottom rows, right figures). The DDCS and TDCS spectra are shown as a function of scattering angle, vertical axis, and approximate energy loss, horizontal axis. Note that in Fig. 1, the electron detector is located above the beam axis. Therefore positive scattering angles, defined to be above the beam axis, correspond to events where both
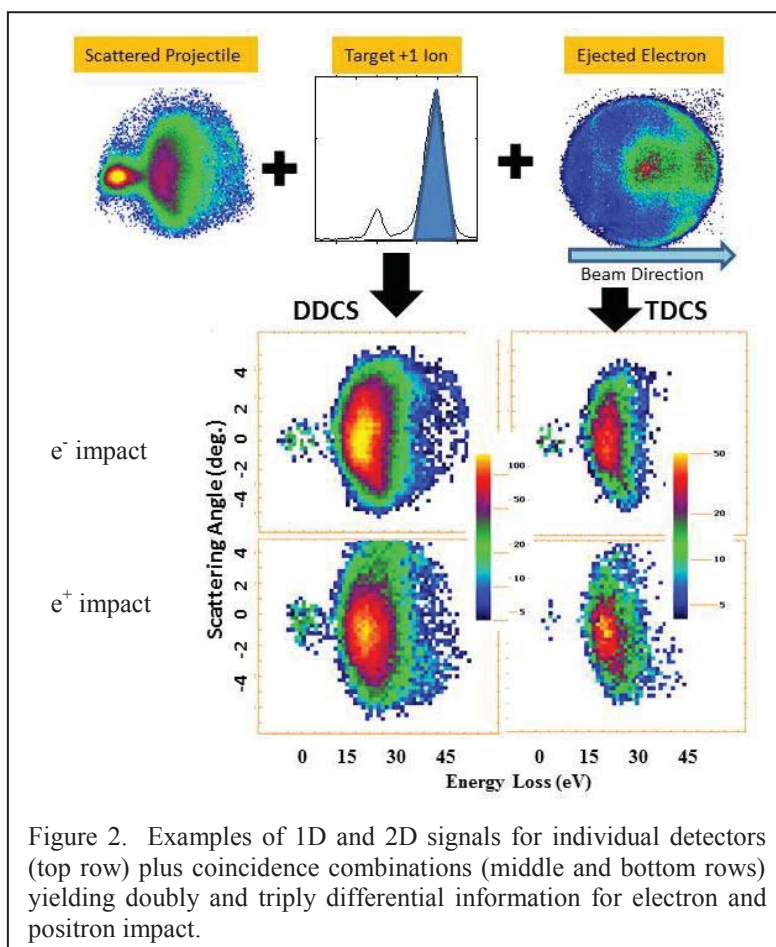

Figure 2. Examples of 1D and 2D signals for individual detectors (top row) plus coincidence combinations (middle and bottom rows) yielding doubly and triply differential information for electron and positron impact.

the scattered projectile and ejected electron are in the same hemisphere relative to the beam axis, i.e., to recoil events. Binary events correspond to negative scattering angles, meaning the projectile scatters down and the electron is ejected up.

In displaying these spectra, because the total cross sections are nearly identical at this impact energy, the electron and positron impact DDCS integral number of counts were normalized to each other and identical color intensity scales (5-150 and 5-50 logrithmetic for the DDCS and TDCS figures) are used, making a simple visual comparison possible. Doing so shows little difference in the electron and positron impact DDCS. However, in the TDCS spectra there is a clear enhancement for negative scattering angles with respect to positive scattering angles for positron impact whereas for electron impact the intensities for positive and negative scattering angles appear to be nearly the same.

3. Results and Progress

3.1. Energy loss studies

Our initial efforts concentrated on measuring single and multiple ionization as a function of energy loss [5,6]. This was done via coincidences between scattered projectiles and target ions, as illustrated by the green box and arrows in Fig. 1. For our first studies, a post collision focusing field was used to extend the maximum scattering angle to ~15°. In more recent studies, no post-collision field is used in order to also obtain information differential in scattering angle. Fig. 3 shows examples of these data for positron and electron impact on argon. The left part compares single and double ionization for 200 eV while the right part shows single ionization data for a higher energy, 1000 eV. At both impact energies, the integral number of single ionization counts are normalized to each other since the total

cross sections are identical. Also, for both examples the scattering angles are small, 0 to ~3°. At 200 eV the positron and electron impact single ionization curves are identical from threshold to approximately a 50 eV (~25%) energy loss after which the yields for electron impact become larger than for positron impact. At 1000 eV the electron impact yields are again larger for energy losses exceeding ~20%. But now distinct differences for smaller energy losses are seen. Namely the initial increase above threshold is notably faster for electron impact and the maximum is significantly broader for positron impact. This broader maximum results in larger yields for positron impact for intermediate energy losses. Although we observe similar differences for 250 eV impact on molecular
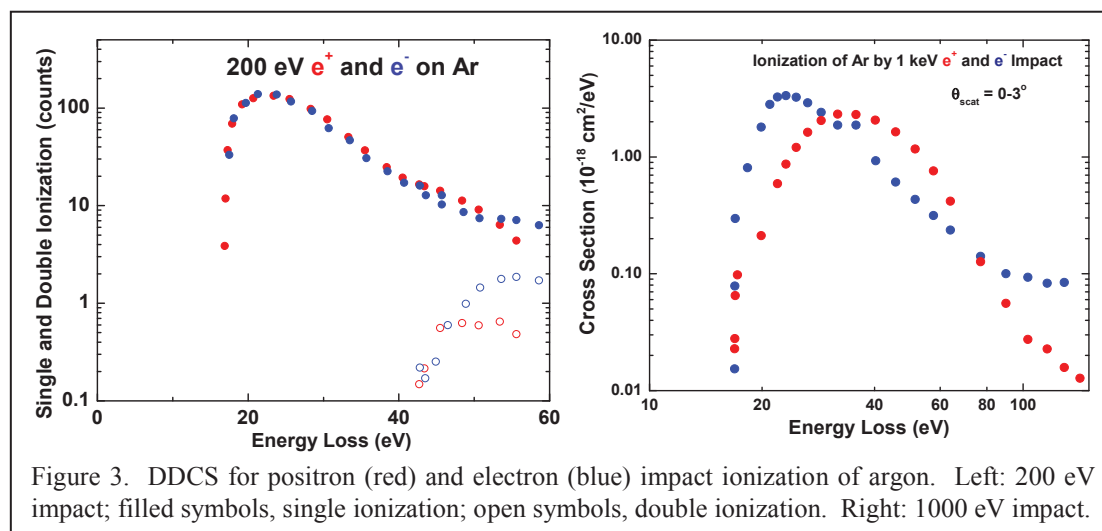

Figure 3. DDCS for positron (red) and electron (blue) impact ionization of argon. Left: 200 eV impact; filled symbols, single ionization; open symbols, double ionization. Right: 1000 eV impact.

nitrogen, a word of caution is needed with regard to differences from threshold and around the maxima. Our use of large beam diameters means that the finite beam width leads to a range of energy losses at each point on our scattered projectile detector. Thus, for small energy losses a deconvolution in order to determine the "mean energy loss" at each energy loss point is necessary. For higher impact energies where the energy loss per pixel is larger, this deconvolution extends over a greater range of energy losses. An additional problem in the threshold region arises for electron impact because of the higher beam intensity. This causes larger random backgrounds that must be removed. Both of these could possibly influence the spectra and lead to differences seen near threshold for the 1000 eV data. However, we again note that we observe similar feature for 250 eV impact where the deconvolution has much less influence.

The left figure also shows double ionization data where, in accordance with total cross section measurements, the electron impact yields are significantly larger. A more extensive comparison of double ionization is shown in the left part of Fig. 4 using data we measured a decade ago for 750 eV e⁺ and e⁻ impact double ionization of argon. As seen, the relative amount of double ionization increases with energy loss in the threshold region then reaches a plateau. For small energy losses, the electron impact ratios are larger than for positron impact but with increasing energy loss, the electron and positron impact ratios merge. The increase around 250 eV, most easily seen in the electron impact data, is due to opening the L-shell Auger double ionization channel.

As stated in the introduction, for double ionization different channels can contribute and interfere. The standard theoretical interpretation [1] assumes the major contributing channels are a first-order project-target electron interaction, either shake off, SO, where a high-energy transfer ejects one electron and the abrupt change in potential leads to emission of a second electron, or 2 step-1, TS1, where a low-energy transfer ejects one electron and, as this electron exits, it knocks out a second electron, and a second-order interaction, TS2, where the projectile interacts with and ionizes each electron independently. Interference between the first- and second-order channels increases the double ionization for negatively charged projectiles and decreases it for positively charged projectiles [1].

Our initial impression was that our energy loss data are consistent with this model since the total cross sections are dominated by small momenta transfer where our ratios are larger for electron impact. However, also shown in the figure are ratios for photo double ionization [7], the solid green curve, which are
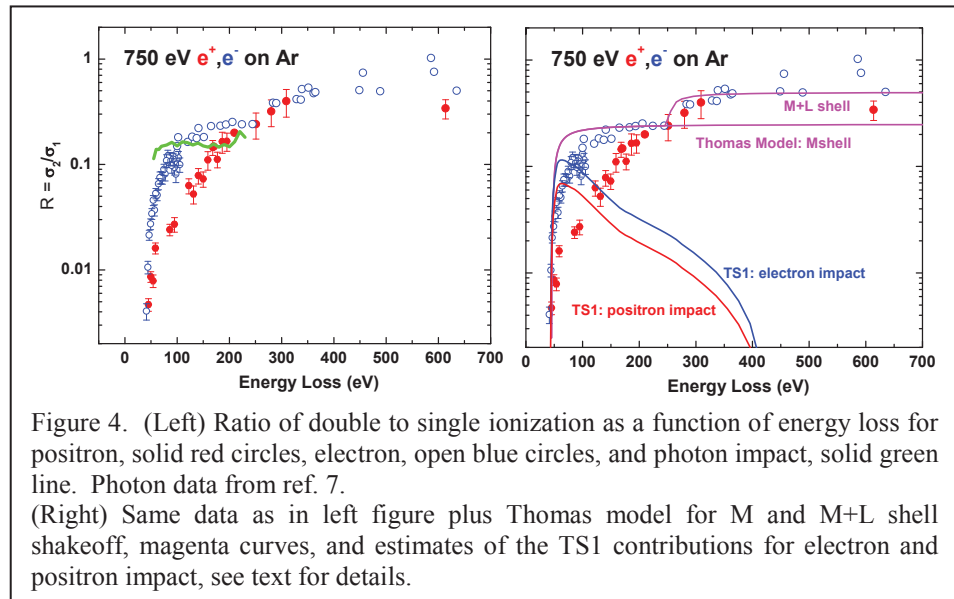

Figure 4. (Left) Ratio of double to single ionization as a function of energy loss for positron, solid red circles, electron, open blue circles, and photon impact, solid green line. Photon data from ref. 7.
(Right) Same data as in left figure plus Thomas model for M and M+L shell shakeoff, magenta curves, and estimates of the TS1 contributions for electron and positron impact, see text for details.

more nearly in agreement with our electron impact data rather that falling somewhere between the electron and positron impact data as expected by the first-order, second-order interference model. We noted this inconsistency a decade ago, but were unable to offer an explanation until recently when we returned to this problem.

Our explanation has several untested premises, but all premises are based on physical processes. Our first premise is that both first-order processes, SO and TS1, are active. Our second premise is that in the TS1 process the second interaction, namely where the first ionized electron interacts with and ionizes the second electron, needs to be included. Doing so will introduce a phase difference between the second electron emission in the SO and TS1 channels because of the finite "transit time" between the first and second ionizations in the TS1 channel. As a result, these first-order channels interfere but now, assuming the same transit times for both positron and electron impact, the interference term does not depend on the projectile charge as was the case for interference between a first- and second-order mechanism. To explain the observed differences between positron and electron impact, we assume that the second step TS1 amplitude is larger for electron impact than for positron impact, our third premise. A possible reason for this is that when the second collision occurs the projectile is still in the vicinity. This means that to be ejected the second electron must overcome the combined fields of the target and the projectile. The net field is reduced for electron impact and increased for positron impact. Our final premise, based upon the energy dependences of the double ionization ratios for proton and antiproton impact, is that first-order processes dominate for Z=1 projectiles with the TS2 second-order process playing a minor role. Justification for these premises is based, in part, upon the right figure in Fig. 4 and, in part, from an analysis of total cross section data.

Based upon these premises, estimates for the SO and TS1 contributions to the energy loss data in Fig. 4 were obtained as follows. The contribution from shake off is obtained from the Thomas model [8] which is regularly used in photon impact double ionization studies. This model gives the SO probability as a function of excess energy above threshold, $P_{SO}(\varepsilon)$, in terms of the shake energy, ΔE, which here is the second ionization potential for outer shell double ionization, ε, the energy transfer minus the ionization potential, and the probability for very large energy transfers, $P_{SO}(\infty)$. The Thomas formula is

$$P_{SO}(\varepsilon) = P_{SO}(\infty) \exp\left(\frac{-m_e r^2 \Delta E^2}{2\hbar^2 \varepsilon}\right)$$

(1)

In the right portion of Fig. 4, we use this formula to determine the SO contributions for double electron removal from the M and L shells of argon. For this, $P_{SO}(\varepsilon)$ was determined simply via

normalization to the energy loss data at large energy losses. For electron impact, this model is in good agreement above ~200 eV energy loss. For smaller energy losses, the Thomas model is known to give values larger than experiment even though the dominant process in the threshold region, TS1, is neglected. We clearly see this in Fig. 4.

To determine the TS1 contributions, we used a modification of the method introduced by Samson [9,10]. Samson noted that the second step of TS1 is essentially electron impact single ionization of a singly charged ion. Therefore he obtained TS1 double ionization ratios using experimental data for electron impact ionization of an ion ($e^- + A^+ \rightarrow 2e^- + A^{++}$) divided by a simple formula for estimating single ionization. We used the same approach using electron impact ionization of Ar^+ data of Müller et al. [11] but added a modification overlooked by Samson. This modification is that simply using the electron impact ionization of an ion data neglects the fact that in the second step of TS1 the "projectile electrons" are secondary electrons produced in the first step. This means that the their number is not constant as in the $e^- + A^+$ data but decreases with increasing secondary electron energy. Therefore, in Fig. 4, the electron impact TS1 contribution, blue curve, was obtained by convoluting the electron impact ionization of Ar^+ data of Müller et al. [11] with secondary electron yields for electron impact[12]. To estimate the TS1 contribution for positron impact, the red curve, the electron results are simply divided by 2, in accordance with differences found in total cross data. It is seen that these TS1 contributions have the qualitative features seen in the threshold region while the SO curves agree with our data for large energy losses. A further refinement of this model where the net fields of the target nucleus and the projectile are modelled and interference between the SO and TS1 channels is estimated, our second and third premises, is currently in progress. Preliminary results of including these show that the electron and positron impact TS1 curves in Fig. 4 will decrease by approximately 10% and a factor of 3 respectively thus giving reasonable quantitative agreement between our *ad hoc* model and experiment.

3.2. TDCS studies

Our initial objective in this project was to measure and compare fully differential data for positron and electron impact. Experimentally, this is done via a triple coincidence measurement of the scattered projectile, the ejected electron, and the recoil ion as illustrated by the blue box and arrows in Fig. 1. Then, by selecting a small range of energy losses and scattering angles for both positive and negative scattering angles and resorting the 2D ejected electron spectra, traditional TDCS for different energy loss, scattering angle, e.g., momenta transfer, conditions can be obtained. A few years back we reported our first TDCS measurements for single ionization of argon [13] and later for ionization of molecular nitrogen [4]. We were able to confirm theoretical predictions [see 13, for example] that the binary and recoil intensities depend on the sign of the projectile charge.

However, our studies to date have not been able to perform the quantitative tests of theory or to help determine which theoretical approach is best or where the available models require improvement. This is because experimentally our current apparatus becomes less and less sensitive for electron emission in the forward and backward directions and is unable to provide information for angles smaller than 30°, between 150 and 210°, or larger than 330°. The decreasing sensitivity results from a
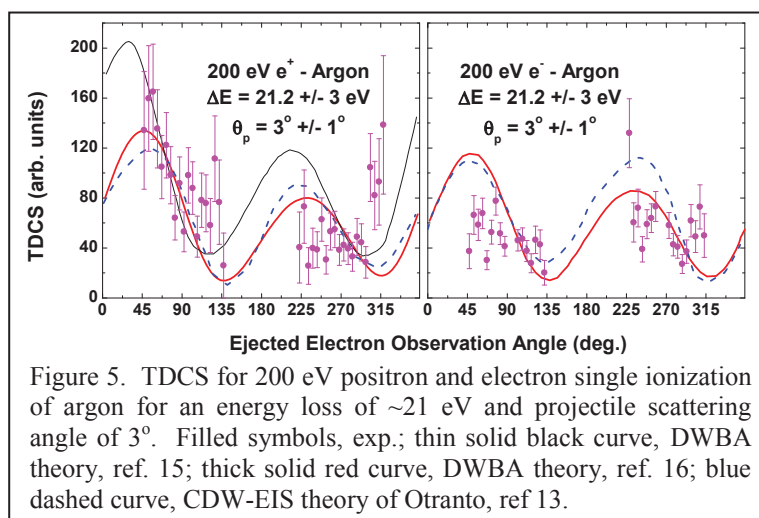

Figure 5. TDCS for 200 eV positron and electron single ionization of argon for an energy loss of ~21 eV and projectile scattering angle of 3°. Filled symbols, exp.; thin solid black curve, DWBA theory, ref. 15; thick solid red curve, DWBA theory, ref. 16; blue dashed curve, CDW-EIS theory of Otranto, ref 13.

combination of the small electric field in the interaction region, the extended beam target overlap volume, and having the electron detector placed close to the interaction region. These introduce significant decreases in detection efficiencies due to the grid transmission and changes in solid angle at small and large angles. We have simulated these changes using a detailed model of the target region geometry and electric fields. This, in principle, allows us to correct the data. However, at our extreme angles significant uncertainties are introduced, making it difficult to draw conclusions when comparing with theory. An additional problem associated with testing theory is the limited statistics for the positron data, e.g., data collection times of 2-3 months non-stop are typical. Finally, a normalization is necessary to compare theory and experiment and precisely where this normalization is made influences which theory agrees best.

These difficulties are shown in Fig. 5 our TDCS measurements for 200 eV positron and electron impact on argon are compared with three available theories [13,15,16]. As seen for positron impact, the three theoretical approaches differ most for angles where experimental information is lacking. Plus, for the comparison shown, theory and experiment were normalized together at 60° for positron impact and should a different normalization be used, which theoretical curve appears best will change. The data do confirm, however, the larger binary to recoil intensities predicted by theory for positron impact and roughly equal intensities for electron impact.

In order to better test theory, we have constructed a new apparatus. This apparatus, shown schematically in Fig. 6, overcomes the lack of, or limited quality, data in the extreme forward and backward direction by adding a second ejected electron detector below the beam axis and rotating the upper and lower detectors as much as possible. Doing so extends the range of electron emission angles significantly plus reduces corrections associated with grid transmission and solid angle. In addition, to reduce the electric field effects for low energy electron emission, the recoil ion detector is rotated
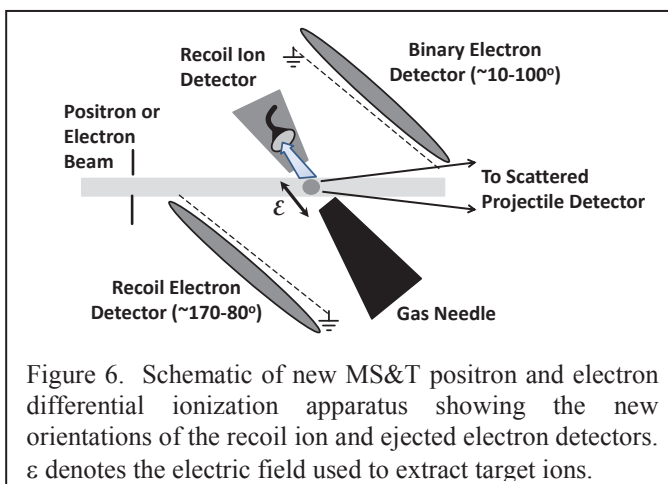

Figure 6. Schematic of new MS&T positron and electron differential ionization apparatus showing the new orientations of the recoil ion and ejected electron detectors. ε denotes the electric field used to extract target ions.

and moved closer to the gas jet and the extraction field is applied only over the very small region where the beam and gas jet overlap. This apparatus has been installed and is currently being tested.

We have used another method to investigate the binary and recoil intensities more closely. Here, identical angular slices of the TDCS and the DDCS 2D spectra shown in Fig. 2 are made for different energy losses. To achieve higher sensitivity and to remove any possible experimental problems associated with particle
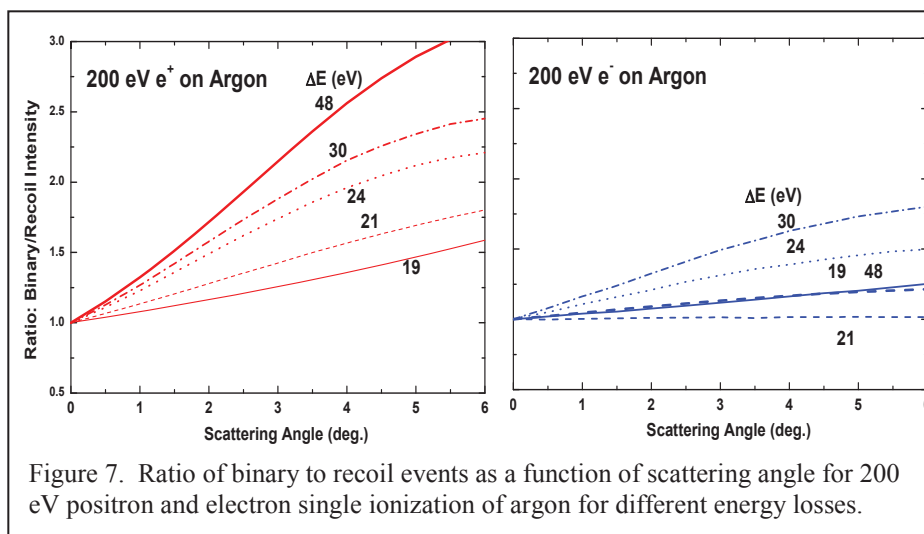

Figure 7. Ratio of binary to recoil events as a function of scattering angle for 200 eV positron and electron single ionization of argon for different energy losses.

transmission or detection at positive and negative scattering angles, TDCS/DDCS ratios are then compared. These ratios show that the relative importance of binary events steadily increases as a function of scattering angle whereas for recoil events little change occurs. In addition, these ratios also show a more isotropic binary and recoil behaviour for electron impact in contrast to the strong increase in the binary intensity with increasing scattering angle for positron impact. To illustrate these features, in Fig. 7 we plot the binary intensities divided by the recoil intensities for positron impact, left figure, and for electron impact, right figure. With increasing energy loss, there is a noticeable monotonic increase in binary events with respect to recoil events for positron impact. In contrast, for electron impact, binary and recoil events are more equally probable, and whether there is a similar monotonic increase as for positron impact is uncertain from the data shown.

4. Summary

Progress in the experimental program at the Missouri University of Science and Technology to investigate differences between positron and electron impact ionization of atoms has been described. Examples of highly differential data ranging from doubly to fully differential data were used to illustrate differences we are observing for single and double ionization. For single ionization, doubly differential data shows the ionization yields to be larger for electron impact when the energy loss is larger than roughly 25% of the beam energy; for smaller energy losses in certain cases the yields for positron and electron impact are identical in other cases differences are noted. Fully differential data for single ionization shows clear differences, namely for positron impact the probability for binary events is significantly larger than for recoil events and increases both as a function of scattering angle and energy loss. In contrast, for electron impact binary events tend to be only slightly more probable than recoil events and the increase with scattering angle is much smaller. For double ionization, electron impact is approximately a factor of 2 more efficient than positron impact. Energy loss measurements indicate that this difference results primarily via the TS1 channel.

References

[1]   McGuire, J H 1982 *Phys. Rev. Lett.* **49** p 1153
[2]   Kirchner, T and Knudsen, H 2011 *J. Phys. B: At. Mol. Opt. Phys.* **44** p 122001
[3]   DuBois, R D, de Lucio, O G and Santos, A C F 2008 *Book chapter in Radiation Physics Research Progress, ed. by Aidan N. Camilleri, (Nova Publishers), ISBN 1-60021-988-8*
[4]   DuBois, R D 2012 *New J. Phys.* **14** p 025004
[5]   DuBois, R D, Doudna, C, Lloyd, C, Kahveci, M, Khayyat, Kh, Zhou, Y and Madison, D H 2001 *J. Phys.* B **34** pp L783-9
[6]   Santos, A C F, Hasan, A, Yates, T and DuBois, R D 2003 *Phys. Rev. A* **67** p 052708
[7]   Holland, D M P, Codling, K, West, J B and Marr, G V 1979 *J. Phys. B* **12** p 2465
[8]   Thomas, T Darrah 1984 *Phys. Rev. Lett.* **52** p 417
[9]   Samson, J A R 1990 *Phys. Rev. Lett.* **65** p 2861
[10]   Samson, J A R, Bartlett, R J, He, Z X 1992 *Phys. Rev. A* **46** p 7277
[11]   Müller, A, Huber, K, Tinschert, K, Becker, R and Salzborn, E 1985 *J. Phys. B: At. Mol. Phys.* **18** p 2993
[12]   DuBois, R D 1975 *Ph.D Thesis, University of Nebraska-Lincoln*
[13]   de Lucio, O G, Otranto, S, Olson, R E and DuBois, R D 2010 *Phys. Rev. Lett.* **104** p 163201
[14]   Campeanu, R I and Alam, M 2011 *Journal ofPhysics:ConferenceSeries* **262** p 012010
[15]   Purohit, G, Patidar, Vinod and Sud, K K 2011 *Nucl. Instr. and Meth. in Phys. Res. B* **269** p 745